

Langmuir–Blodgett Monolayers of Gold Nanoparticles with Amphiphilic Shells from V-Shaped Binary Polymer Arms

Kirsten L. Genson,[†] Jason Holzmüller,[†] Chaoyang Jiang,^{†,§} Jun Xu,[†] Jacob D. Gibson,[‡] Eugene R. Zubarev,[‡] and Vladimir V. Tsukruk^{*,†,§}

Department of Materials Science and Engineering, Iowa State University, Ames, Iowa 50011, School of Materials Science and Engineering, Georgia Institute of Technology, Atlanta, Georgia 30332, and Department of Chemistry, Rice University, Houston, Texas 77005

Received April 28, 2006. In Final Form: June 5, 2006

Gold nanoparticles functionalized with amphiphilic polybutadiene–poly(ethylene glycol) (PB–PEG) V-shaped arms formed stable Langmuir monolayers at the air–water and the air–solid interfaces. At these interfaces, the binary arms vertically segregated into a dense polymer corona, which surrounded the gold nanoparticles, preventing their large-scale agglomeration and keeping individual nanoparticles well-separated from each other and forming flattened, pancake nanostructures. The presence of both PEG and PB chains in the close proximity to the gold core was confirmed by surface enhanced Raman spectroscopy, whereas the AFM phase contrast images revealed the presence of 2 nm gold cores surrounded by the polymer shell with the diameter of 11 nm. We suggest that the amphiphilic shell drives their spontaneous organization into discrete 2D pancakelike hybrid structures that measured up to 10 μm in diameter and had a high packing density of gold clusters.

Introduction

Nanoparticles of noble metals with different dimensionalities and surface functionalities are attractive targets for numerous technological and biomedical applications due to their unusual magnetic, optical, electronic, and catalytic properties.^{1–6} Controlled ordering of inorganic species at the interfaces is a challenging goal, which requires their high packing density without an irreversible agglomeration. Organic–inorganic hybrid structures combine the attractive properties of the metallic nanoparticle core with interparticle distances and ordering controlled by the protecting polymeric shell. The “polymer nanotemplating” approach creates defined nanoscale architectures by nucleating inorganic crystals within a polymer matrix.^{7–10} For example, hybrid building blocks composed of 3.2 nm diameter gold nanoparticles encapsulated in PAMAM dendrimers have been observed to self-organize on the amphiphilic patterned surfaces.^{11,12} A similar approach of encapsulating Cu, Pd, and Pt nanoparticles in PAMAM dendrimers was demonstrated by Zhao and Crooks.^{13–15}

As was suggested, the functionalization of small inorganic nanoparticles with long polymeric brushes would isolate the inorganic core from the environment and develop the hybrid materials with novel properties. Indeed, gold nanoparticles have been physically encapsulated in cross-linked diblock copolymer micelles, eliminating the need for linking moieties.¹⁶ Such amphiphilic copolymers are known to drive ordering at the air–water interface and in selective solvents and thus can be explored to control interfacial behavior of metal nanoparticles if used as a shell component.^{17–21} On the other hand, it was demonstrated that mixed Langmuir monolayers of surfactants and ligand-stabilized metal–core nanoclusters formed highly ordered nanostructured films.^{22–24} However, to date, no examples of inorganic nanoparticles encapsulated into responsive shells capable of changing their properties under external stimuli (e.g., variation of solvent polarity) have been demonstrated.

Therefore, this study examines stimuli-responsive gold nanoparticles functionalized with amphiphilic binary corona composed of V-shaped polymer arms chemically grafted to the gold surface. We focus on determining the molecular dimensions and interfacial ordering of these core–shell nanoparticles at the air–water and air–solid interfaces. The presence of hydrophobic and hydrophilic

* Corresponding author. E-mail: vladimir@iastate.edu.

[†] Iowa State University.

[‡] Rice University.

[§] Georgia Institute of Technology.

(1) Hammond, P. T. *Adv. Mater.* **2004**, *16*, 1271.

(2) Goodson, T.; Varnavski, O.; Wang, Y. *Int. Rev. Phys. Chem.* **2004**, *23*, 109.

(3) Eychmüller, A. *J. Phys. Chem. B* **2000**, *104*, 6514.

(4) Chiu, J. J.; Kim, B. J.; Kramer, E. J.; Pine, D. J. *J. Am. Chem. Soc.* **2005**, *127*, 5036.

(5) Xia, Y.; Gates, B.; Yin, Y.; Lu, Y. *Adv. Mater.* **2000**, *12*, 693.

(6) (a) Jiang, C.; Tsukruk, V. V. *Adv. Mater.* **2006**, *18*, 829. (b) Luzinov, I.; Minko, S.; Tsukruk, V. V. *Prog. Polym. Sci.* **2004**, *29*, 635. (c) Jiang, C.; Tsukruk, V. V. *Soft Matter* **2005**, *1*, 334.

(7) Antonietti, M.; Goltner, C. *Angew. Chem., Int. Ed.* **1997**, *36*, 910.

(8) Antonietti, M.; Grohn, F.; Hartmann, J.; Bronstein, L. *Angew. Chem., Int. Ed.* **1997**, *36*, 2080.

(9) Balogh, L.; Tomalia, D. A. *J. Am. Chem. Soc.* **1998**, *120*, 7355.

(10) Esumi, K.; Suzuki, A.; Yamahira, A.; Torigoe, K. *Langmuir* **2000**, *16*, 2604.

(11) Grohn, F.; Gu, H.; Grull, H.; Mededith, J. C.; Nisato, G.; Bauer, B. J.; Karim, A.; Amis, E. J. *Macromolecules* **2002**, *35*, 4852.

(12) Grohn, F.; Bauer, B. J.; Akpalu, Y. A.; Jackson, C. L.; Amis, E. J. *Macromolecules* **2000**, *33*, 6042.

(13) Zhao, M.; Sun, L.; Crooks, R. M. *J. Am. Chem. Soc.* **1998**, *120*, 4877.

(14) Zhao, M.; Crooks, R. M. *Adv. Mater.* **1999**, *11*, 217.

(15) Zhao, M.; Crooks, R. M. *Angew. Chem., Int. Ed.* **1999**, *38*, 364.

(16) Kang, Y.; Taton, T. A. *Angew. Chem., Int. Ed.* **2005**, *44*, 409.

(17) (a) Shan, J.; Nuopponen, M.; Jiang, H.; Viitala, T.; Kauppinen, E.; Kontturi, K.; Tenhu, H. *Macromolecules* **2005**, *38*, 2918. (b) Shan, J.; Chen, J.; Nuopponen, M.; Viitala, T.; Jiang, H.; Peltonen, J.; Kauppinen, E.; Tenhu, H. *Langmuir* **2006**, *22*, 794.

(18) Swami, A.; Kumar, A.; Selvakannan, P. R.; Mandal, S.; Sastry, M. J. *Colloid Interface Sci.* **2003**, *260*, 367.

(19) Fendler, J. H.; Meldum, F. *Adv. Mater.* **1995**, *7*, 607.

(20) Brown, J. J.; Porter, J. A.; Daghighian, C. P.; Gibson, U. J. *Langmuir* **2001**, *17*, 7966.

(21) Liu, J.; Alvarez, J.; Ong, W.; Roman, E.; Kaifer, A. E. *J. Am. Chem. Soc.* **2001**, *123*, 11148.

(22) Khomutov, G. B.; Kislov, V. V.; Gainutdinov, R. V.; Gubin, S. P.; Obydenov, A. Yu.; Pavlov, S. A.; Sergeev-Cherenkov, A. N.; Soldatov, S. A.; Tolstikhina, A. L.; Trifonov, A. S. *Surf. Sci.* **2003**, *532*–535, 287.

(23) Zubilov, A. A.; Gubin, S. P.; Korotkov, A. K.; Nikolaev, A. G.; Soldatov, E. S.; Khanin, V. V.; Khomutov, G. B.; Yakovenko, S. A. *Tech. Phys. Lett.* **1994**, *20*, 195.

(24) Khomutov, G. B.; Soldatov, E. S.; Gubin, S. P.; Yakovenko, S. A.; Trifonov, A. S.; Obydenov, A. Yu.; Khanin, V. V. *Thin Solid Films* **1998**, *327*–329, 550.

polymer chains chemically grafted to a single joint facilitates the formation of stable Langmuir monolayers and fine structural ordering within the monolayers caused by vertical segregation of dissimilar arms and the formation of pancake nanostructures.

The branched binary gold nanoparticles reported here expand a series of highly branched binary star-copolymers introduced earlier, which demonstrated peculiar amphiphilic behavior with strongly segregated nanophase structures.²⁵ The advantage of this system is the well-defined structure (PDI = 1.07 by GPC) and exact 1:1 molar ratio of hydrophilic PEG and hydrophobic PB chains attached to a given gold core. This is due to the synthetic strategy used for the preparation of this material when pre-synthesized carboxyl-terminated V-shaped PB-PEG block copolymer molecules are covalently attached to hydroxyl-functionalized gold nanoparticles via an ester linkage as discussed in detail elsewhere.²⁶ This is a significant advantage over the systems prepared by reacting a mixture of two thiolated polymers upon reduction of gold and the approach of chemically grafting monolayers from pre-assembled binary brush molecules on a planar substrate.²⁷

Experimental Section

The gold nanoparticles with amphiphilic V-shaped arms were synthesized as described in detail elsewhere.²⁸ The V-shaped amphiphilic molecule containing a hydrophilic poly(ethylene glycol) PEG₄₅ ($M_w = 2200$) and hydrophobic 1,4-polybutadiene PB₂₀ ($M_w = 1000$) was attached covalently to 2 nm mercaptophenol-derivatized gold nanoparticles via ester linkage, forming a dense shell (Figure 1). Monomolecular films from these molecules were prepared by the Langmuir technique on an RK-1 trough (Riegel & Kirstein, GmbH) according to the usual procedure adapted in our lab.^{29,30} The trough was placed in a laminar flow hood. The compound studied here was dissolved in chloroform (Fisher, ACS reagent grade) at ~ 0.01 mmol/L concentration. The solution was spread over the water subphase (NanoPure, > 18 M Ω cm) and dried for 30 min before compression. Monomolecular films were deposited on cleaned silicon substrates (Semiconductor Processing Co.) using the Langmuir-Blodgett (LB) technique. Freshly prepared silicon wafers were treated in "piranha" solution (30% hydrogen peroxide:94% sulfuric acid, 1:3, *chemical hazard!*) according to the standard procedure.³¹

Atomic force microscopic (AFM) imaging of the LB monolayers was performed with AFM microscopes, Dimension-3000 and Multimode (Digital Instruments), in the light tapping mode according to an experimental procedure described elsewhere.³²⁻³⁴ Raman spectroscopy was conducted with a custom-designed instrument based on an Aurora-III near-field scanning optical microscope (Digital Instruments).³⁵ A Nd:YAG (yttrium aluminum garnet) laser (532 nm) was used as the light source, with an intensity of 1 mW. The

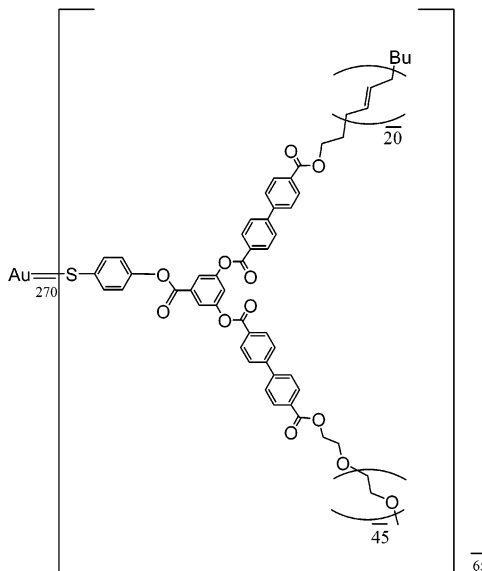


Figure 1. Chemical formula of a single V-shaped molecule attached to a gold core of Au(PB-PEG)_n nanoparticles.

spectra were recorded by a cooled charge-coupled device (CCD) camera with resolution of 0.32 cm⁻¹. Transmission electron microscopy (TEM) images were obtained on a JEOL 2010 microscope operating at 120 kV. The samples were prepared by casting a drop of 0.1 wt % THF solution on carbon-coated copper grid followed by drying at room temperature for 3 h before imaging. The geometrical parameters of all molecules were estimated from molecular models built with the Materials Studio 3.0 software package and the Cerius² program on a SGI workstation. The combination of molecular dynamics and force-field energy minimization was used to generate molecular models before taking molecular dimensions.

Results and Discussion

Surface Behavior at the Air-Water Interface. Initial GPC analysis performed for the molecules studied here estimated only 6 V-shaped molecules attached to the gold core. However, this technique is known to significantly underestimate the molecular weight of branched structures as was previously demonstrated for high generation dendrimers and star-shaped polymers.³⁶ Therefore, on the basis of high-resolution TEM images and the elemental analysis, it was estimated that approximately 65 V-shaped molecules were tethered to a given Au NP as discussed in detail earlier.²⁸

The extended diameter of Au(PB-PEG)_n hybrid molecules with the given composition was calculated to be about 30 nm with each V-shaped molecule measuring 13 nm in a fully extended conformation (Figure 2, top). However, the collapse of the polymer arms to form a dense shell surrounding the gold nanoparticle core (e.g. in a bad solvent like air) should reduce the overall molecular diameter to 13 nm as depicted schematically in Figure 2, bottom. The "stiff" core of the compound composed of the gold nanoparticle and phenylbenzoate fragments possesses a diameter of about 6 nm and occupies about 1/8 of the total volume with 7/8 of the volume representing the polymer shell occupied by flexible arms.

The grafting density of the V-shaped molecules onto gold surface for these core-shell nanoparticles is extremely high,

(25) Genson, K. L.; Hoffman, J.; Teng, J.; Zubarev, E. R.; Vaknin, D.; Tsukruk, V. V. *Langmuir* **2004**, *20*, 9044.

(26) Xu, J.; Zubarev, E. R. *Angew. Chem., Int. Ed.* **2004**, *43*, 5491.

(27) (a) Julthongpipit, D.; Lin, Y.-H.; Teng, J.; Zubarev, E. R.; Tsukruk, V. V. *Langmuir* **2003**, *19*, 7832. (b) Julthongpipit, D.; Lin, Y.-H.; Teng, J.; Zubarev, E. R.; Tsukruk, V. V. *J. Am. Chem. Soc.* **2003**, *125*, 15912. (c) Lin, Y.-H.; Teng, J.; Zubarev, E. R.; Shulha, H.; Tsukruk, V. V. *Nano Lett.* **2005**, *5*, 491. (d) LeMieux, M. C.; Lin, Y.-H.; Cuong, P. D.; Ahn, H.-S.; Zubarev, E. R.; Tsukruk, V. V. *Adv. Funct. Mater.* **2005**, *15*, 1529.

(28) Zubarev, E. R.; Xu, J.; Sayyad, A.; Gibson, J. D. *J. Am. Chem. Soc.* **2006**, *128*, 4958.

(29) Peleshanko, S.; Sidorenko, A.; Larson, K.; Villavicencio, O.; Ornatka, M.; McGrath, D. V.; Tsukruk, V. V. *Thin Solid Films* **2002**, *406*, 233.

(30) Sidorenko, A.; Houphouet-Boigny, C.; Villavicencio, O.; McGrath, D. V.; Tsukruk, V. V. *Thin Solid Films* **2002**, *410*, 147.

(31) Tsukruk, V. V.; Bliznyuk, V. N.; Hazel, J.; Visser, D.; Everson, M. P. *Langmuir* **1996**, *12*, 4840.

(32) Tsukruk, V. V. *Rubber Chem. Technol.* **1997**, *70*, 430.

(33) Tsukruk, V. V.; Reneker, D. H. *Polymer* **1995**, *36*, 1791.

(34) Ratner, B.; Tsukruk, V. V., Eds. *Scanning Probe Microscopy of Polymers*; ACS Symposium Series; American Chemical Society: Washington, DC, 1998; Vol. 694.

(35) Ko, H.; Pikus, Y.; Jiang, C.; Jauss, A.; Hollricher, O.; Tsukruk, V. V. *Appl. Phys. Lett.* **2004**, *85*, 2598.

(36) (a) Mourey, T. H.; Turner, S. R.; Rubinstein, M.; Frechet, J. M. J.; Hawker, C. J.; Wooley, K. L. *Macromolecules* **1992**, *25*, 2401. (b) Xu, Z. F.; Moore, J. S. *Angew. Chem., Int. Ed.* **1993**, *32*, 1354.

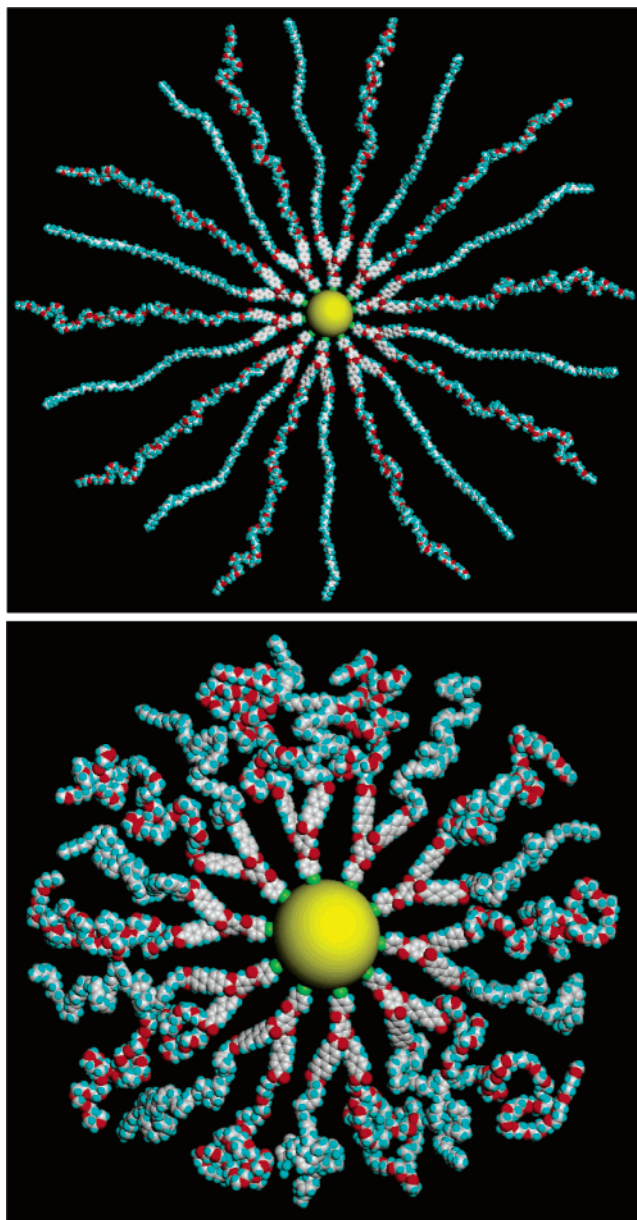


Figure 2. Molecular model of gold nanoparticles with amphiphilic binary shells with extended (above) and collapsed polymeric arms (below). For clarity, only ten attached molecules are included. White, carbon; blue, hydrogen; red, oxygen; and green, sulfur.

reaching 0.2 nm^2 per a V-shaped molecule. This value reaches the limits of the dense packing of phenylbenzoate groups in the upright orientation and indicates very dense packing of V-shaped junctions in the vicinity of the gold surface with more space available for packing of polymer chains in the outer shell. The estimated grafting density for these molecules is much higher than that usually observed for polymer chains chemically grafted to a planar substrate.^{27,37} However, for nanoparticles with small diameters, it has been demonstrated that steric constraints in the lateral packing of polymer chains within curved shells are much removed due to an additional free volume provided by highly curved grafting surfaces for outer shells, thus allowing the surface area per a single molecule to reach $0.18\text{--}0.24 \text{ nm}^2$.³⁸

(37) Luzinov, I.; Julthongpipit, D.; Malz, H.; Pionteck, J.; Tsukruk, V. V. *Macromolecules* **2000**, *33*, 1043.

(38) Corbierre, M. K.; Cameron, N. S.; Lennox, R. B. *Langmuir* **2004**, *20*, 2867.

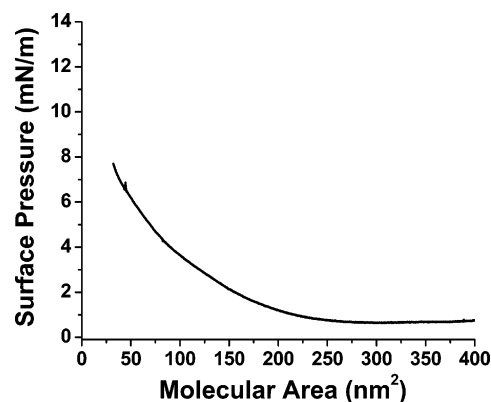


Figure 3. The π - A isotherm of $\text{Au}(\text{PB-PEG})_n$ nanoparticles at modest lateral compression.

The $\text{Au}(\text{PB-PEG})_n$ hybrid nanoparticles with both hydrophilic and hydrophobic arms comprising a polymer shell formed stable Langmuir monolayers at the air-water interface with reversible compression behavior at modest surface pressures reaching 10 mN/m (Figure 3). The Langmuir monolayer was compressed irreversibly and collapses at higher lateral compression with the surface pressure reaching 18 mN/m (not shown). The molecular area that corresponded to an initial slight rise in the surface pressure was estimated to be within $200\text{--}250 \text{ nm}^2$ per molecule. On the other hand, the cross-sectional area per molecule in the condensed monolayer determined from the rise in the surface pressure was close to 140 nm^2 (Figure 3). Finally, the limiting cross-sectional area for the reversible compression was close to 50 nm^2 with the smallest cross-sectional area preceding the monolayer collapse at 30 nm^2 .

The detectable surface pressure increase observed below 250 nm^2 fell between the maximum cross-sectional area of the compound with completely extended arms ($\sim 500 \text{ nm}^2$) and that in the partially collapsed state with coiled conformation of flexible arms (140 nm^2) (Figure 2). In this state, the PEG chains can be partially adsorbed at the air-water interface and partially submerged in the water subphase. Considering that the surface packing density in this loose state should not exceed 60%, the estimated molecular area of 230 nm^2 fits closely to the onset of the surface pressure increase. The following rise in the surface pressure for the molecular areas below 150 nm^2 reflects the formation of the more condensed Langmuir monolayers with diminishing molecular areas associated with gradual submerging of the hydrophilic PEG arms into the water subphase. This behavior is similar to that reported before for star and branched molecules containing a variable number of PEG arms varying from 2 to 18.³⁹

Finally, a sharp precollapsed rise in the surface pressure can be associated with direct lateral contact of rigid cores (30 nm^2 per molecule) of gold nanoparticles with attached rigid fragments after all hydrophilic arms completely submerged in the water subphase. In this state, the hydrophobic arms should vertically segregate above the water surface, a common phenomenon for PEO-containing star-block copolymers.^{39,40} The highest reachable surface pressure in our case is well below that usually observed for amphiphilic star-copolymers, which can be caused by a disturbance introduced into in-plane packing by the core-shell

(39) (a) Peleshanko, S.; Gunawidjaja, R.; Jeong, J.; Shevchenko, V. V.; Tsukruk, V. V. *Langmuir* **2004**, *20*, 9423. (b) Peleshanko, S.; Jeong, J.; Shevchenko, V. V.; Genson, K. L.; Pikus, Y.; Petrash, S.; Tsukruk, V. V. *Macromolecules* **2004**, *37*, 7497. (c) Gunawidjaja, R.; Peleshanko, S.; Genson, K. L.; Tsitsilianis, C.; Tsukruk, V. V. *Langmuir* **2006**, *22*, 6168.

(40) Peleshanko, S.; Jeong, J.; Gunawidjaja, R.; Tsukruk, V. V. *Macromolecules* **2004**, *37*, 6511.

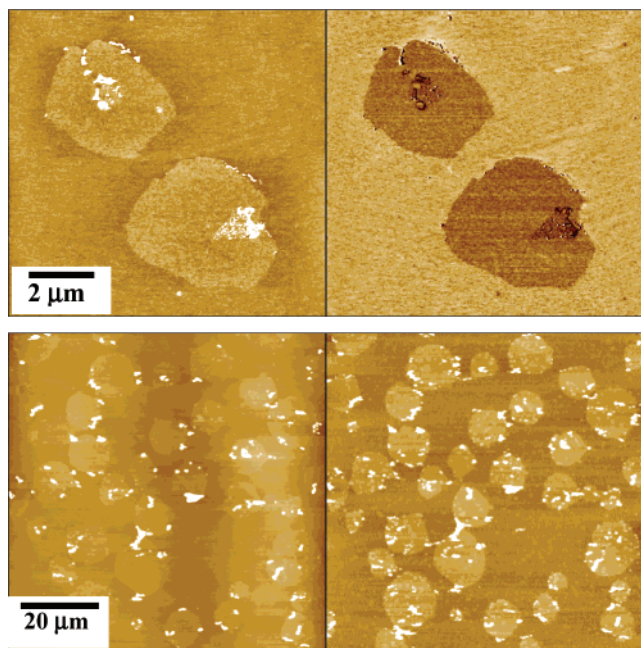


Figure 4. AFM topographical (left) and phase (right) images of the LB monolayer deposited at 5 mN/m at different magnifications. The Z scales are 5 nm and 20° for upper images, and 20 nm and 20° for lower ones.

structure as well as a nonuniform monolayer morphology (heterogeneous domain microstructure) (see below).

Surface Morphology of LB Monolayers. A well-defined domain structure was confirmed for the LB monolayers deposited at low and medium surface pressures. The Au(PB-PEG)_n molecules formed very large round domains (the diameter varying from 4 to 10 μm) at all molecular areas studied here (Figure 4). The number of circular domains rose for the monolayer deposited at the lowest cross-sectional area, resulting in their denser packing. A thin underlying monolayer was observed to spread between the domains, suggesting the two-phase monolayer structure usually observed in the condensed liquid state and the expanded solid state of Langmuir monolayers where two types of molecular packings coexist in a wide range of pressures.^{41,42} More densely packed planar domains with slightly increased thickness are formed within laterally compressed regions. Comparison of the domain height versus the gold nanoparticle core diameter further supported this conclusion. The average height of the domains modestly increased from 0.4 ± 0.1 nm for monolayers deposited at lower pressure to 0.6 ± 0.1 nm for monolayers deposited at the highest surface pressure. This difference suggests that the domains are composed of molecules with PB chains vertically segregated and spread at the air-layer surface rising above molecules with horizontally spread arms, thus generating the overall pancake shapes in the selected surface areas.

The pancake shape of the core-shell nanoparticles at the interfaces and the vertical segregation of the hydrophobic chains into a dense corona surrounding the gold nanoparticle core were confirmed by high-resolution AFM images for domain surface areas. As was observed, the Au(PB-PEG)_n molecules formed a fine dimpled texture within the circular 2D nanostructures (Figure 5). A similar texture with slightly large circular nanostructures was observed for the underlying layer at the surface

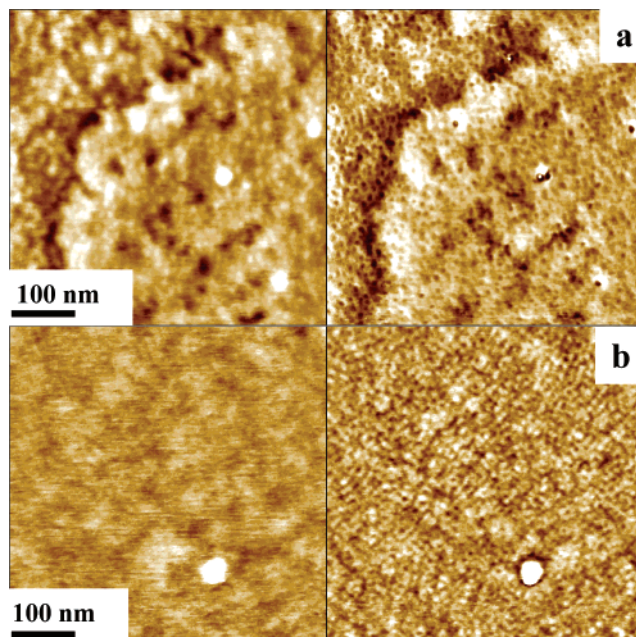


Figure 5. High-resolution AFM topographical (left) and phase (right) images for the LB monolayer deposited at 5 mN/m demonstrating compressed and expanded ringlike structures: the domain edge (a) and the underlying layer (b). The Z scales for images (a) are 2 nm and 5°, and 3 nm and 5° for (b).

areas surrounding the domains. The phase contrast of the dimpled structure showed a ringlike surface structure with the significant phase contrast between cores and rims, suggesting a gold core ringed by the aggregated polymer corona. From high-resolution AFM images, we calculated the ring diameter by exploiting the cross-sectional analysis and taking into account the AFM tip shape as discussed in a number of previous publications.⁴³ Moreover, for ringlike structures with elevated rims and depressed cores, the influence of the AFM tip is minimal as discussed in our previous studies.^{27,32,44} The diameter of 11 ± 1.5 nm measured for the monolayers was close to the diameter of the molecular model when the polymer corona densely packed around the gold core and hydrophobic chains aggregated above the overall surface (Figure 2).

Further evidence of the possibility for dense but nonaggregated surface packing of Au(PB-PEG)_n was obtained from TEM experiments (Figure 6). When a molecular film of nanoparticles is deposited onto a carbon-coated grid, one can observe a dense packing of dark dots measuring ~2 nm, which represent the metallic cores of the hybrid Au(PB-PEG)_n structures. The dots are separated by the polymeric shell, which creates a light gray background because the polymer arms scatter electron density to a much lower extent. The apparent interparticle distance varies from 6 to 8 nm, which is somewhat smaller than the average interparticle distance observed in the AFM images in laterally compressed monolayers. However, the molecular film prepared by casting a dilute solution onto carbon support may have contained more than a single molecular layer in some areas. The overlap of several layers would diminish the average interparticle distance when viewed in 2D projection. However, the overall

(41) (a) Gaines, G. L., Jr. *Insoluble Monolayers at Liquid-Gas Interfaces*; Interscience: New York, 1966. (b) Ulman, A. *Introduction to Ultrathin Organic Films*; Academic Press: San Diego, 1991.

(42) (a) Kaganer, V. M.; Möhwald, H.; Dutta, P. *Rev. Mod. Phys.* **1999**, *71*, 779. (b) Peterson, I. R. *J. Phys. D: Appl. Phys.* **1990**, *23*, 379.

(43) (a) Ratner, B., Tsukruk, V. V., Eds. *Scanning Probe Microscopy in Polymers*; ACS Symposium Series; American Chemical Society: Washington, DC, 1998; Vol. 694. (b) Tsukruk, V. V., Wahl, K., Eds. *Microstructure and Microtribology of Polymer Surfaces*; ACS Symposium Series; American Chemical Society: Washington, DC, 2000; Vol. 741. (c) Tsukruk, V. V., Spencer, N. D., Eds. *Advances in Scanning Probe Microscopy of Polymers. Macromol. Symp.* **2001**, *167*. (d) Tsukruk, V. V. *Adv. Mater.* **2001**, *13*, 95.

(44) Holzmueller, J.; Genson, K. L.; Park, Y.; Yoo, Y.-S.; Park, M.-H.; Lee, M.; Tsukruk, V. V. *Langmuir* **2005**, *21*, 6392.

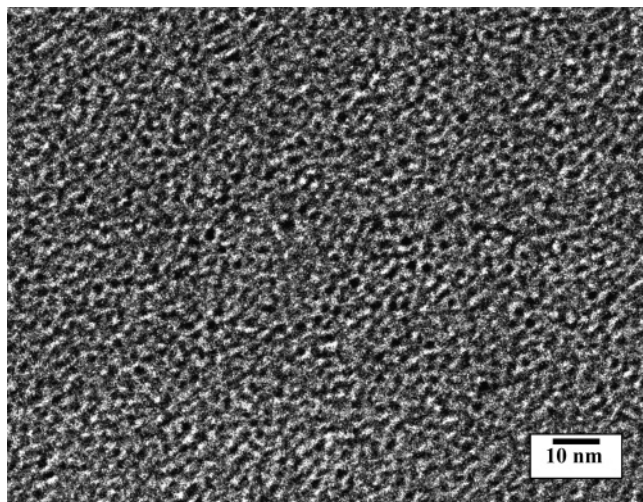


Figure 6. TEM image of Au(PB-PEG)_n nanoparticles cast from THF solution on a carbon-coated TEM grid.

appearance and the high packing density of the hybrid Au(PB-PEG)_n structures observed by TEM are very similar and consistent with the dimpled surface nanostructures found in high-resolution AFM images.

Raman Scattering for Au(PB-PEG)_n Monolayers. We were able to confirm the chemical composition of the amphiphilic structures in the monolayers with Raman spectroscopy and reveal additional features of intramonolayer molecular packing. The presence of gold nanoparticles was vital in this experiment because for a single monolayer with similar composition and thickness Raman scattering is extremely weak and is well below any sensitivity limits preventing any detection. However, as known, noble metal nanostructures can be responsible for a tremendous increase in Raman scattering cross-section. These nanostructures are widely applied as active fillers or substrates to enhance the Raman scattering and facilitate surface-enhanced Raman scattering (SERS) phenomenon.⁴⁵ SERS makes it possible to study microstructures and molecular orientations down to a single molecule resolution.^{46,47} Considering the inclusion of gold nanoparticles with a very small diameter into LB monolayers, we expected to observe SERS signals for the Au(PB-PEG)_n monolayer, but even in the case of LB monolayers with similar thickness the Raman signal cannot be detected.

Indeed, a series of strong Raman peaks was observed for the Au(PB-PEG)_n LB monolayer despite its minute overall thickness (about 2 nm), which usually makes it impossible to observe any Raman signal (Figure 7). The presence of gold nanoparticles facilitated the observation of characteristic adsorption Raman bands for both PEG and PB chains due to the SERS phenomenon. The positions of different bands were analyzed by using literature data for Raman spectra of similar compounds.⁴⁸ A strong peak caused by the silicon substrate was also observed (Figure 7). The

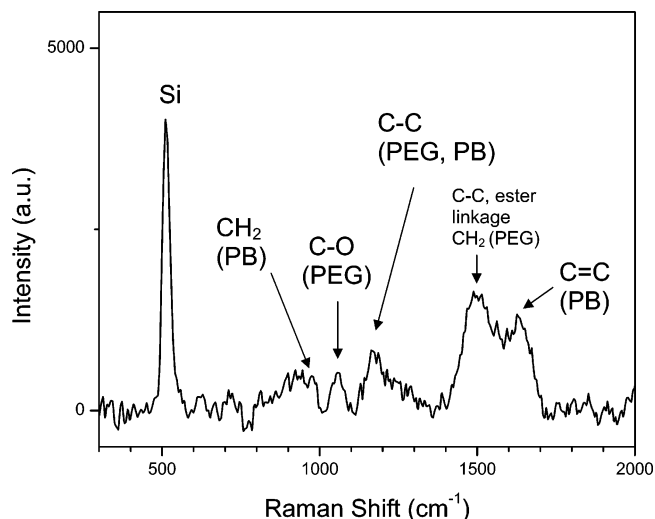


Figure 7. Raman spectrum of Au(PB-PEG)_n LB monolayer with major bands assigned to specific vibrational modes.

strongest Raman peak at 1488 cm^{-1} can be assigned to a CH₂ scissor vibration of PEG chains according to the literature sources as well as C-C stretching for the benzene rings of the V-shaped fragment (Figure 1).^{47,49} Another peak that belongs to PEG is near 1058 cm^{-1} . This peak is related to C-O bond vibration in the PEG backbone.⁴⁹ The broad peak at 1156 cm^{-1} is associated with C-C stretching of both PEG and PB backbones.^{49,50} Finally, the peaks at 1665 and 964 cm^{-1} correspond to C=C stretching and CH₂ rock vibrations of PB backbones, respectively.⁵⁰

An even enhancement of Raman bands that belong to two different arms is a strong indication of their equal and close proximity to the gold surface. To obtain significant SERS phenomenon, this distance should be within 2–4 nm.⁵¹ This result rules out the model of arms arrangement within the outer shell with a preferential segregation of one type of the arms in the vicinity of the gold core. In contrast, this result strongly supports the model of vertical segregation of dissimilar arms and the formation of the pancake nanostructures as suggested above from AFM data. For such segregation, both types of arms form thin layers above and below the gold nanoparticles, thus providing a chance for significant and comparable portions of their segments to be in close proximity to the gold surface, which is possible only for vertically segregated hydrophilic and hydrophobic arms in the outer shells of hybrid nanoparticle structures.

Acknowledgment. We thank Srikanth Singamaneni for technical assistance. Funding from the National Science Foundation (DMR-038982 and CTS-NIRT-0506832) and AFOSR F496200210205 grants is gratefully acknowledged.

LA061163P

(45) Cao, Y. C.; Jin, R.; Mirkin, C. A. *Science* **2002**, *297*, 1536.

(46) Tian, Z.-Q.; Ren, B.; Wu, D.-Y. *J. Phys. Chem. B* **2002**, *106*, 9470.

(47) Jiang, C.; Lio, W. Y.; Tsukruk, V. V. *Phys. Rev. Lett.* **2005**, *95*, 115503.

(48) (a) Larsson, M.; Lu, J.; Lindgren, J. *J. Raman Spectrosc.* **2004**, *35*, 826.

(b) Sokolov, K.; Chumanov, G.; Cotton, T. M. *Anal. Chem.* **1998**, *70*, 3898. (c)

Loa, I. *J. Raman Spectrosc.* **2003**, *34*, 611.

(49) Koenig, J. L.; Angood, A. C. *J. Polym. Sci., Part A: Polym. Chem.* **1970**, *8*, 1787.

(50) Hsu, S. L.; Moore, W. H.; Krimm, S. *J. Appl. Phys.* **1975**, *10*, 4185.

(51) Sarychev, K. A.; Shalaev, V. M. *Phys. Rep.* **2000**, *335*, 275.